SIAM J. APPL. MATH.
Vol. 65, No. 6, pp. 1839–1854

CHANNEL FORMATION IN GELS*

N. G. COGAN† AND JAMES P. KEENER‡

Abstract. We derive and give an analysis of a model of gel dynamics based on a two-phase description of the gel, where one phase consists of networked polymer and the second phase is the fluid solvent. It is found that for the gel to maintain an edge in a poor solvent, the function describing the osmotic pressure must be of a particular form. The model is used to study the behavior of a gel forced by a pressure gradient to move between two flat plates. The distribution of the network phase under these conditions is found to be nonuniform and dependent on the pressure gradient. There is a range of pressure gradients for which the network has regions of high and low volume fraction separated by a sharp boundary, indicative of a channel. We provide the bifurcation analysis of how these novel, singularly perturbed, channeled solutions occur.

Key words. gel, model, viscoelasticity, osmotic pressure, biofilm

AMS subject classifications. 74D99, 74G10, 76T99

DOI. 10.1137/040605515

1. Introduction.

There are numerous biological and biotechnological examples where the structure and dynamics of polymer gels regulates the local environment. Biological examples include maintenance of structural integrity in biofilms [8], cellular cytoplasm [3], force generators in myxobacteria [14], and chemical diffusion and adsorption mediation in biofilm clusters [12]. Gel patches and ingestible pills used to regulate the diffusion and adsorption of drugs are examples of bioengineered gels. Quantifying the role of the polymer gel in such diverse systems requires understanding the effect of the physical and chemical structure of the polymers on the material properties of the system.

Gels are composed of a polymer network and a fluid solvent. This composition endows gels with properties different than those of viscous materials for two primary reasons. First, the polymeric structure induces viscoelastic behavior. Second, the chemical structure of the polymer induces force, causing gel swelling and deswelling. In this paper we first introduce a two-phase description of gel dynamics that emphasizes these two important differences between gels and Newtonian fluids. The behavior of a pressure driven gel between two flat plates is analyzed in a manner similar to the standard Poiseulle flow problem. Results from this analysis indicate that the steady-state network profile depends on the pressure gradient in a relatively complicated manner. There is an intermediate range of pressure gradients for which the majority of the network is compressed and located near the plates, creating a channeled region which is relatively free of polymer. This channeled solution arises via a novel bifurcation mechanism from a nearly uniform network distribution by forming a deep, narrow channel.

2. A model of gel dynamics.

Gels consist of two materials, networked polymer and fluid solvent, where the network encapsulates the solvent. The polymer

*Received by the editors March 23, 2004; accepted for publication (in revised form) December 27, 2004; published electronically August 3, 2005. This work was supported in part by NSF-FRG grant DMS 0139926.

http://www.siam.org/journals/siap/65-6/60551.html

†Department of Mathematics, Tulane University, New Orleans, LA (cogan@math.tulane.edu).

‡Department of Mathematics, University of Utah, Salt Lake City, UT (keener@math.utah.edu).

network can be formed by several different interactions between the polymers themselves including covalent bonding, coulombic bonding, hydrogen bonding, and physical entanglement.

In response to external conditions, gel networks absorb or expel solvent, causing swelling or contraction, respectively. Thus the structure of the gel depends on the temperature, solvent composition, pH, hydrostatic pressure, and ionic concentrations. The potential which is responsible for the swelling properties of the gel is referred to as osmotic or swelling pressure.

Forces due to osmotic pressure are not the only forces acting on the polymer network. Deformation of the gel induces forces due to the elastic nature of the polymer network. The elasticity is caused by both the elasticity of the polymers themselves and polymer interactions. That is, a single polymer acts as a spring for small deformations, while entanglement and cross-linking cause the network to resist deformations. The behavior is in general not well described by a simple linear relationship between displacement (strain) and stress primarily because the deformations are typically large.

Because the cross-links may be broken, a strain imposed on the gel and held induces a stress which dissipates, a process referred to as relaxation. Further, if a fixed stress is imposed on the gel, the gel will continue to displace, which is referred to as creep. The two behaviors of creep and relaxation indicate that gels are viscoelastic materials; therefore the constitutive relationship between stress and strain is typically more complicated than for viscous materials.

Here we assume that a gel is composed of two immiscible materials, polymer network and fluid solvent. The resulting model is similar to other models [3, 6, 9, 11, 13] that describe the gel as a two-phase material. The primary variation among models in the literature results from the treatment of the viscoelastic stress and the swelling pressure. In this study, we will neglect the relaxation of the network and assume that the gel is composed of an elastic solid (network) embedded in a viscous fluid (solvent). The swelling pressure is specified to ensure that physically reasonable swelling/deswelling is reflected in the deformation process.

In the following sections we describe a general model of gel dynamics and specify the forms of the viscoelastic stress and osmotic pressure used in this investigation. The resulting model is then used to study the distribution of the polymer network when the gel is forced to move between two flat plates by a pressure gradient.

2.1. Model derivation. We consider a region of space that contains networked polymer and solvent, where the volume fraction of network, θ_n, and the volume fraction of solvent, θ_s, sum to one. The network is assumed to act as a constant density viscoelastic material, while the solvent acts as a Newtonian fluid of much less viscosity than the networked material. The velocities of network and solvent are denoted $\vec{U}_n$ and $\vec{U}_s$, respectively.

The equation describing the momentum of the polymer network is given by the balance of four forces that act on the network. Surface forces are given by $\nabla \cdot (\theta_n \sigma_n)$, where σ_n is the network stress tensor. We assume that $\sigma_n = \sigma_v + \sigma_e$, where the viscous and elastic stresses are denoted σ_v and σ_e, respectively. The viscous stress tensor is proportional to the velocity gradient, $\sigma_v = \frac{\eta}{2}(\nabla \vec{U}_n + \nabla \vec{U}_n^T)$. The non-Newtonian stress tensor is given by constitutive relations which depend on the material and flow regimes [1]. Here we take the elastic stress to be proportional to the elastic strain, which is determined by the displacement gradient. We do not allow for creep or relaxation of stress. Thus, we are describing the deformation process of the moving gel. Since the displacements are not small, we use a finite strain tensor. The displacement of a fluid

particle relative to fixed Eulerian coordinates is determined by

$$\vec{x}' = \vec{x} + \vec{D}(\vec{x}, t),$$

where $\vec{x}'$ denotes the past position of the fluid particle and the components of the vector $\vec{D}$ are the displacements.

Following the development given in [1], the stress is related to the strain through

$$\sigma_e = \gamma \mathbf{C}, \tag{1}$$

where $\mathbf{C}$ is the relative Cauchy strain tensor

$$\mathbf{C}(\vec{x}, t)_{i,j} = \mathbf{F}_{ji}\mathbf{F}_{ij} - \delta_{ij},$$

with $\mathbf{F}_{ij} = \frac{\partial x_i'}{\partial x_j} = \frac{\partial D_i}{\partial x_j} + \delta_{ij}$ the deformation gradient tensor and $\delta_{ij} = 0$ if $i \neq j$, $\delta_{ii} = 1$.

We must also specify equations describing the change in displacements due to advection. The time derivative is measured in convected coordinates (i.e., relative to a fixed coordinate system). We assume that the gel is an elastic solid with rest position at which there is no network strain, while displacements from rest induce a strain on the network. Relaxation of the network has been ignored since we are primarily interested in coupling between elastic stress and network motion. Thus

$$\frac{\partial}{\partial t}\vec{D} + \nabla \cdot (\vec{D}\vec{U}_n) = \vec{U}_n. \tag{2}$$

The motion of the solvent influences the network through frictional drag, which we model by $h_f\theta_n\theta_s(\vec{U}_n - \vec{U}_s)$, where $\vec{U}_n$ and $\vec{U}_s$ are the network and solvent velocities and h_f is the constant coefficient of friction.

The third force is induced by the chemically active nature of the polymers within the gel. To model this force, we assume that there exists an osmotic pressure, $\Psi(\theta)$, gradients of which induce force on the polymers. Additional description of this term is provided below.

The final force that is included is due to hydrostatic pressure, P. Balancing all these forces yields

$$\begin{aligned}\nabla \cdot (\theta_n\sigma_n) - h_f\theta_n\theta_s(\vec{U}_n - \vec{U}_s) \\ - \nabla\Psi(\theta_n) - \theta_n\nabla P = 0.\end{aligned} \tag{3}$$

The equation governing the solvent momentum is derived in a similar manner. However, the fluid is chemically passive so there is no osmotic force on the solvent and the stress is Newtonian. Force balance yields

$$\nabla \cdot (\theta_s\sigma_s) + h_f\theta_n\theta_s(\vec{U}_n - \vec{U}_s) - \theta_s\nabla P = 0, \tag{4}$$

where $\sigma_s = \frac{\eta_s}{2}(\nabla\vec{U}_s + \nabla\vec{U}_s^T)$.

Notice that (3) and (4) are very similar to the Stokes equation for incompressible flows at zero Reynolds number. In particular, by neglecting the inertial terms, we are assuming that the system responds instantaneously to applied forces.

The redistribution of the polymer network is governed by the conservation equation

$$\frac{\partial}{\partial t}\theta_n + \nabla \cdot (\theta_n\vec{U}_n) = 0, \tag{5}$$

and a similar equation governs the conservation of solvent, namely,

$$\frac{\partial}{\partial t}\theta_s + \nabla \cdot (\theta_s \vec{U}_s) = 0. \tag{6}$$

Assuming that $\theta_n + \theta_s = 1$, we combine (5) and (6) to conclude that the divergence of the average flow, $\theta_n \vec{U}_n + \theta_s \vec{U}_s$, is zero; i.e.,

$$\nabla \cdot (\theta_n \vec{U}_n + \theta_s \vec{U}_s) = 0. \tag{7}$$

Equations (2), (3), (4), (5), and (7) govern the gel dynamics, subject to boundary conditions which depend on the specific problem. Throughout this paper, it will be useful to allow for diffusive smoothing of the network. This can be motivated physically by the fact that there is probably a small amount of polymeric diffusion within the gel. It is also useful from a mathematical perspective because it guarantees that solutions are smooth, even if there are sharp transitions. This modification yields the equation

$$\frac{\partial}{\partial t}\theta_n + \nabla \cdot (\theta_n \vec{U}_n) = \epsilon \nabla^2 \theta_n \tag{8}$$

for the redistribution of polymer network, and

$$\nabla \cdot (\theta_n \vec{U}_n + \theta_s \vec{U}_s) = \epsilon \nabla^2 \theta_n \tag{9}$$

for the incompressibility condition.

2.2. Osmotic pressure. Although there are many models of gel dynamics in the literature which include terms representing osmotic pressure [2, 3, 6, 7, 10, 11, 13], there is little agreement on either the definition or the derivation of this term. The treatment of this term varies from qualitative [3, 6] to quantitative [13]. In [7, 10, 11] a specific functional form of the osmotic pressure is not given. In fact, there has been little investigation of the dynamic behavior using different forms of the swelling pressure. Therefore our first task is to determine a model of swelling pressure which reflects some experimental results. Specifically, in many experiments a blob of gel is suspended in a solvent, causing the gel to swell. The amount of swelling is a measure of the effectiveness of the solvent. In general, the gel does not completely dissolve; instead, the blob swells a certain amount and then persists with a lower volume fraction, maintaining a distinct interface between the gel and the surrounding solvent.

We wish to determine what choice of Ψ, if any, allows for the existence of an edge between the gel and the surrounding solvent. To do so, we examine the solution of a simplified one-dimensional model of network redistribution due to swelling pressure alone. In the absence of elastic restoring force ($\sigma_e = 0$), network motion is governed by the balance of forces due to viscous stress, osmotic pressure, and hydrostatic pressure. Considering the steady-state problem implies that $\vec{U}_s = 0$ (from (5)). Using (4) to eliminate P from (3), the time independent one-dimensional equations governing network distribution are

$$\eta \frac{d}{dx}\left(\theta_n \frac{dV_n}{dx}\right) = h_f \theta_n V_n + \frac{d}{dx}\Psi(\theta_n), \tag{10}$$

$$\frac{d}{dx}(\theta_n V_n) = \epsilon \frac{d^2 \theta_n}{dx^2}, \tag{11}$$

where V_n is the x-component of $\vec{U}_n$. To be physically relevant, the solution should persist in the limit $\epsilon \to 0$.

The boundary conditions for this system are that $V_n = 0$ and there is no network flux $\epsilon \frac{d\theta_n}{dx} = \theta_n V_n$ at $x = 0$ and $x = L$, where L is the length of the one-dimensional spatial domain. This second condition allows us to integrate (11) and then substitute the result into (10), and also integrate this to find the second order system of equations

$$\eta \frac{dV_n}{dx} = \epsilon h_f + \frac{\Psi(\theta_n)}{\theta_n} + \frac{k}{\theta_n}, \tag{12}$$

$$\epsilon \frac{d\theta_n}{dx} = \theta_n V_n. \tag{13}$$

This is a singularly perturbed system. We want there to be solutions $\theta_n = 0$ and $\theta_n = \theta_{ref}$ which exist in the limit $\epsilon \to 0$ and which also can be connected by a transition layer. For $\theta_n = \theta_{ref}$ to be a solution, it must be that $k + \Psi(\theta_{ref}) = 0$, and for $\theta_n = 0$ to be a solution, it must be that

$$\lim_{\theta_n \to 0} \frac{\Psi(\theta_n)}{\theta_n} + \frac{k}{\theta_n} = 0. \tag{14}$$

It follows that

$$\Psi(\theta_n) = -k + \theta_n^2 f(\theta_n), \tag{15}$$

where $f(\theta_{ref}) = 0$. Of course, we can take $k = 0$, since only the gradient of Ψ appears in the governing equations.

Now we seek a transition layer that connects the two solutions $\theta_n = 0$ and $\theta_n = \theta_{ref}$. In this transition layer it must be that (ignoring the term ϵh_f)

$$\frac{\eta}{\epsilon} \frac{dV_n}{d\theta_n} = \frac{f(\theta_n)}{V_n}, \tag{16}$$

from which it follows that

$$\frac{\eta}{\epsilon} V_n^2 = -\int_{\theta_n}^{\theta_{ref}} f(\theta) d\theta, \tag{17}$$

implying that $f(\theta_n) < 0$ on the interval $0 \le \theta_n \le \theta_{ref}$. In the special case that $f(\theta_n) = \gamma_{os}(\theta_n - \theta_{ref})$, we find that

$$V_n = \pm \sqrt{\frac{\gamma_{os}\epsilon}{\eta}} (\theta_n - \theta_{ref}), \tag{18}$$

with transition layer trajectory satisfying

$$\frac{d\theta_n}{dx} = \pm \sqrt{\frac{\gamma_{os}}{\epsilon\eta}} \theta_n (\theta_n - \theta_{ref}), \tag{19}$$

a hyperbolic tangent solution with boundary layer width the order of $\sqrt{\epsilon}$.

It follows that, for a gel to hold an edge, Ψ must be of the form (up to an arbitrary additive constant) $\Psi(\theta_n) = \theta_n^2 f(\theta_n)$ with $f(\theta_{ref}) = 0$ and $f(\theta_n) \le 0$ for $0 < \theta_n < \theta_{ref}$. A specific example of such a function that we use throughout the rest of this paper is $\Psi(\theta_n) = \gamma_{os}\theta_n^2(\theta_n - \theta_{ref})$.

Having determined the form of the osmotic pressure that allows transition layers between $\theta_n = 0$ and $\theta_n = \theta_{ref}$, we now wish to determine the stability of steady solutions. Notice that any constant $\theta_n = \theta_0$ is a solution of (3), (4), (8), and (9) with $\vec{U}_n = \vec{U}_s = 0$ (provided $\sigma_e = 0$). To study its stability, we linearize the governing equations about this uniform solution (setting $\vec{U}_n = u$, $\vec{U}_s = v$, $\theta_n = \theta_0 + \phi$, $\theta_s = 1 - \theta_0 - \phi$.), to find

$$\frac{\partial \phi}{\partial t} + \nabla \cdot (u\theta_0) = \epsilon \nabla^2 \phi, \tag{20}$$

$$\nabla \cdot (u\theta_0 + v(1-\theta_0)) = \epsilon \nabla^2 \phi, \tag{21}$$

$$\frac{1}{2}\nabla \cdot (\theta_0 \eta(\nabla u + \nabla u^T)) - h_f \theta_0 (u - v) - \Psi'(\theta_0)\nabla\phi = 0. \tag{22}$$

To find the dispersion relation for this problem, we try a solution of the form $\phi = A(t)e^{i\omega\cdot x}$, $u = B(t)e^{i\omega\cdot x}$, $v = C(t)e^{i\omega\cdot x}$, and obtain equations for A, B, and C:

$$\frac{dA}{dt} + i\omega(B\theta_0) = -\omega^2 \epsilon A, \tag{23}$$

$$i\omega(B\theta_0 + C(1-\theta_0)) = -\omega^2 \epsilon A, \tag{24}$$

$$-\omega^2 \theta_0 \eta B - h_f \theta_0 (B - C) - \Psi'(\theta_0) i\omega A = 0. \tag{25}$$

We solve for B and C and substitute into (23) to find

$$C = \frac{i\omega\epsilon A - B\theta_0}{1-\theta_0}, \tag{26}$$

$$B = \frac{\epsilon h_f \theta_0 - (1-\theta_0)\Psi'(\theta_0)}{\omega^2 \theta_0 \eta (1-\theta_0) + h_f \theta_0} i\omega A, \tag{27}$$

$$\frac{dA}{dt} = \omega^2 \frac{\epsilon h_f \theta_0 - (1-\theta_0)\Psi'(\theta_0)}{\omega^2 \eta (1-\theta_0) + h_f} A - \omega^2 \epsilon A. \tag{28}$$

In the limit $\epsilon \to 0$ this is

$$\frac{dA}{dt} = -\omega^2 \frac{(1-\theta_0)\Psi'(\theta_0)}{\omega^2 \eta (1-\theta_0) + h_f} A. \tag{29}$$

Clearly, this is stable if $\psi'(\theta_0) > 0$ and unstable if $\psi'(\theta_0) < 0$.

Thus, for the function $\Psi(\theta_n) = \gamma_{os}\theta_n^2(\theta_n - \theta_{ref})$, a uniform gel with $\theta_n < \gamma_{os}\frac{2}{3}\theta_{ref}$ is unstable, while a uniform gel with $\theta_n > \gamma_{os}\frac{2}{3}\theta_{ref}$ is stable. Thus, very low density gels are not stable and will tend to form deswelled spatially localized aggregates.

3. Channeling behavior. We now turn to a simple problem illustrating one difference between gel dynamics and Newtonian fluid dynamics. We consider the deformation of the network component of a gel which is forced to move between two flat plates due to a constant imposed pressure drop. We make one further assumption that the viscosity of the system is dominated by the network viscosity ($\theta_n \eta \gg \theta_s \eta_s$), and thus, following [13], we neglect the solvent viscosity. Notice that although the solvent is inviscid, the frictional interaction between the solvent and the network still renders the entire system viscous.

The motion is assumed to be two-dimensional, where x, y and $\vec{U}_* = (V_*, W_*)$ denote the horizontal and vertical coordinates and velocities, respectively. For Newtonian fluids the steady-state x independent velocity profile is parabolic in y for all pressure drops. This is not the case for the gel-Poiseulle flow. Instead, the steady-state profile of the network volume fraction undergoes a large change as the magnitude of the pressure gradient varies.

To demonstrate this, we seek a solution of (3)–(7) that is the analogue of Poiseulle flow—the horizontally independent steady velocity profile for a fluid forced between two flat plates by a pressure drop.

Under the assumption that D_1 and D_2 are independent of x, the elements of the deformation gradient tensor $\mathbf{F}_{ij}$ are

$$\begin{aligned} \frac{\partial x'}{\partial x} &= 1, \\ \frac{\partial x'}{\partial y} &= \frac{\partial D_1}{\partial y}, \\ \frac{\partial y'}{\partial x} &= 0, \\ \frac{\partial y'}{\partial y} &= 1 + \frac{\partial D_2}{\partial y}, \end{aligned}$$

and the stress tensor becomes

$$\sigma_e = \gamma \begin{bmatrix} 0 & \frac{\partial D_1}{\partial y} \\ \frac{\partial D_1}{\partial y} & \left(\frac{\partial D_1}{\partial y}\right)^2 + 2\frac{\partial D_2}{\partial y} + \left(\frac{\partial D_2}{\partial y}\right)^2 \end{bmatrix}.$$

We change from vector to component notation here, so that the following simplifications are more apparent. In component form the steady-state equations for the gel-Poiseulle flow are

$$\eta \frac{\partial}{\partial y}\left(\theta_n \frac{\partial}{\partial y} V_n\right) - \frac{\partial P}{\partial x} + \gamma \frac{\partial}{\partial y}\left(\theta_n \frac{\partial}{\partial y} D_1\right) = 0, \tag{30}$$

$$\begin{aligned} \eta \frac{\partial}{\partial y}\left(\theta_n \frac{\partial}{\partial y} W_n\right) - \frac{\partial}{\partial y}\Psi(\theta_n) - \frac{\partial P}{\partial y} \\ + \gamma \frac{\partial}{\partial y}\left(\theta_n \left(\left(\frac{\partial D_1}{\partial y}\right)^2 + 2\frac{\partial D_2}{\partial y} + \left(\frac{\partial D_2}{\partial y}\right)^2\right)\right) = 0, \end{aligned} \tag{31}$$

$$h_f \theta_n (V_n - V_s) - \frac{\partial P}{\partial x} = 0, \tag{32}$$

$$h_f \theta_n (W_n - W_s) - \frac{\partial P}{\partial y} = 0, \tag{33}$$

$$\frac{\partial}{\partial y}(\theta_n W_n + (1 - \theta_n) W_s) = \epsilon \frac{\partial^2 \theta_n}{\partial y^2}, \tag{34}$$

$$\frac{\partial}{\partial y}(\theta_n W_n) = \epsilon \frac{\partial^2 \theta_n}{\partial y^2}, \tag{35}$$

$$\frac{\partial}{\partial y}(D_1 W_n) = V_n, \tag{36}$$

$$\frac{\partial}{\partial y}(D_2 W_n) = W_n. \tag{37}$$

Here we allow for network diffusion, with diffusion coefficient ϵ, but our goal is to solve the system in the limit $\epsilon \to 0$.

The distance between the two plates is taken to be L; hence the domain of the problem consists of an infinite strip $(-\infty < x < \infty) \times (0 < y < L)$. The boundary conditions are $D_1 = D_2 = 0$ and $\epsilon \frac{\partial \theta_n}{\partial y} = \theta_n W_n$ at $y = 0, L$, implying that there is neither network displacement nor network flux at the boundary.

We can simplify these equations substantially. Integrating (35) and solving for the vertical velocity of the network, we find

$$W_n = \epsilon \frac{\frac{\partial \theta_n}{\partial y} + c_1}{\theta_n}, \tag{38}$$

which, combined with (34), yields

$$(1 - \theta_n) W_s = c_2. \tag{39}$$

These can be used in (33) to solve for the $\frac{\partial P}{\partial y}$ as

$$\frac{\partial P}{\partial y} = h_f \theta_n \left(W_n - \frac{c_2}{1 - \theta_n} \right). \tag{40}$$

The boundary conditions imply that $c_1 = c_2 = 0$; hence $W_s = 0$ and $\frac{\partial P}{\partial y} = h_f \epsilon \frac{\partial \theta_n}{\partial y}$. Because $V_n = 0$ at steady state, and because the equations are independent of x, $\frac{\partial P}{\partial x}$ is independent of x. That is, (32) implies that $P = Gx + \hat{P}(y)$.

Integrating (30) and solving for $\frac{\partial D_1}{\partial y}$ yields

$$\frac{\partial D_1}{\partial y} = \frac{Gy + a}{\gamma \theta_n}. \tag{41}$$

We specify a by assuming that the steady-state profiles are symmetric about the center line, $y = \frac{1}{2}$. We also relate the vertical displacements to the network volume fraction using the Jacobian of the transformation

$$\hat{\theta}_n = \theta_n \left(1 + \frac{\partial D_2}{\partial y} \right),$$

where $\hat{\theta}_n$ is the original homogeneous unstressed distribution of the network.

Finally, (31) reduces to an ordinary differential equation (ODE) relating the volume fraction of the network to y and parameters G, γ, h_f, etc.:

$$\begin{aligned} &\epsilon \eta \frac{d}{dy} \left(\theta_n \frac{d}{dy} \left(\frac{\frac{d\theta_n}{dy}}{\theta_n} \right) \right) - \epsilon h_f \frac{d\theta_n}{dy} \\ &- \frac{d\Psi}{dy} + \gamma \frac{d}{dy} \left(\theta_n \left(\left(\frac{Gy - GL/2}{\gamma \theta_n} \right)^2 + \left(\frac{\hat{\theta}_n}{\theta_n} \right)^2 - 1 \right) \right) = 0. \end{aligned} \tag{42}$$

We nondimensionalize (42) by defining the nondimensional variable $y^* = \frac{y}{L}$ and the nondimensional parameters $\epsilon^* = \frac{\eta}{L^2\gamma}\epsilon$ and $h_f^* = \frac{L^2 h_f}{\eta}$, $G^* = \frac{L}{\gamma}G$; substituting these into (42); and dropping the $*$-notation. Integrating once yields

(43)
$$\epsilon\left(\theta_n \frac{d}{dy}\left(\frac{\frac{d\theta_n}{dy}}{\theta_n}\right)\right) - \epsilon h_f \theta_n - \frac{1}{\gamma}\Psi(\theta_n) + \left(\theta_n\left(G^2\left(\frac{y-1/2}{\theta_n}\right)^2 + \left(\frac{\hat{\theta}_n}{\theta_n}\right)^2 - 1\right)\right) = k,$$

which must be solved subject to the constraint that mass is conserved,

$$\int_0^1 \theta_n \, dy = \hat{\theta}_n. \tag{44}$$

Although simpler than the original system, there remains quite a lot of interesting structure in (43). In particular, (43) is a second order ODE which is singular in the limit $\epsilon \to 0$. In the following section, we describe the singular perturbation analysis of this problem, revealing the existence of channels, i.e., solutions with sharp interior transition layers.

3.1. The channeling bifurcation. In this section we analyze the bifurcation structure of channels by examining the solutions of (43) in the singular limit $\epsilon \to 0$. We assume that the initially uniform gel at $\hat{\theta}_n$ is stable so that $\Psi'(\hat{\theta}_n) > 0$.

The reduced equation ($\epsilon = 0$) is an algebraic equation relating the network volume fraction to the location between the plates. The steady state network profile is given by the solution of the algebraic equation

$$H(y, \theta_n) = G^2\left(y - \frac{1}{2}\right)^2 + h(\theta_n) = 0, \tag{45}$$

where

$$h(\theta_n) = -\theta_n\Psi(\theta_n) + \theta_n\Psi(\hat{\theta}_n) + \hat{\theta}_n^2 - \theta_n^2 - k\theta_n, \tag{46}$$

and

$$\Psi(\theta_n) = \kappa\theta_n^2(\theta_n - \theta_{ref}), \tag{47}$$

where $\kappa = \frac{\gamma_{os}}{\gamma}$ represents the strength of osmosis compared to the elastic modulus. Here k has been redefined so that $H(\hat{\theta}_n) = 0$ when $k = 0$. The solution profile $\theta_n(y)$ must also satisfy the integral constraint 44.

By virtue of the form of Ψ, the gel is capable of supporting an edge. In many hydrogels, the polymer network is of very low density and is highly charged [5]. This suggests that the strength of the osmotic pressure is large compared to the magnitude of the elastic modulus, so that κ is large.

This problem can be viewed as a nonlinear eigenvalue problem: "For each value of G determine the value(s) of k for which the solution of (45) satisfies the integral constraint (44)." However, it turns out that it is easier to view the problem as follows: "For each value of k find the value(s) of G for which the solution of (45) satisfies the integral constraint (44)." We explain below why this is the case.

First we make some observations about the function $h(\theta)$. Because $h(0) = \hat{\theta}_n^2 > 0$, and $h(\theta) < 0$ for large θ, $h(\theta)$ always has at least one positive and one negative root.

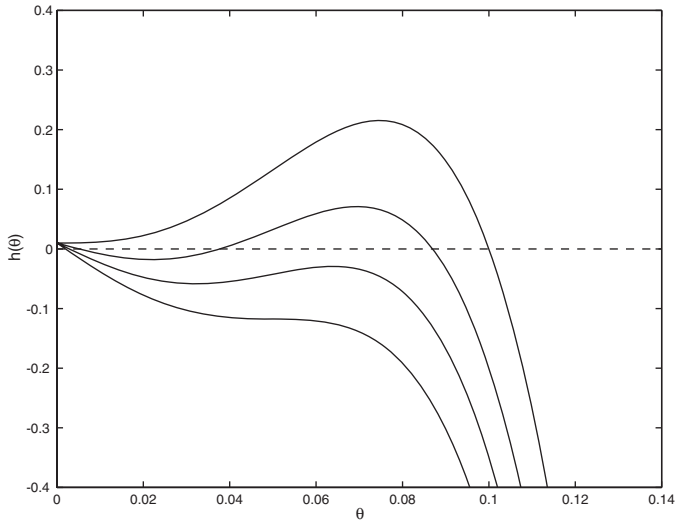

FIG. 1. *Plot of $h(\theta)$ as a function of θ for $k = 0, 2, 3.5, 5$. Other parameter values are $\kappa = 20{,}000$ and $\theta_{ref} = \hat{\theta}_n = 0.1$.*

Since $h(\theta)$ is a quartic polynomial in θ, there can be as many as three positive roots of $H(y, \theta_n) = 0$, depending on the value of k. To see this, in Figure 1 are shown four different plots of $h(\theta)$ for four values of $k = 0, 2, 3.5, 5$ (top to bottom). If $3\kappa\theta_{ref}^2 > 8$, the function $h(\theta)$ has two positive inflection points. Thus, if κ is sufficiently small, the function $h(\theta)$ is monotone for positive θ, whereas, if κ is sufficiently large, it is possible that $h(\theta)$ is nonmonotone.

We seek solutions of (45) that are of the form $\theta_n = \Theta_n(y)$. However, because $h(\theta)$ need not be monotone, such solutions do not always exist. However, it is always possible to write the solution implicitly for y as function of θ_n,

$$y = \frac{1}{2} \pm \frac{1}{G}\sqrt{-h(\theta_n)}. \tag{48}$$

Thus, one can visualize solutions by turning the plots in Figure 1 "on their side." If the resulting solution is single-valued, there is little more to do. If the resulting solution is multivalued, then one must determine which pieces of the multivalued function should be used to construct a single-valued function.

To construct admissible single-valued solutions from multivalued ones, we look for interior transition layers that connect different branches of the multivalued solution. Suppose that at $y = y_0$, $H(y_0, \theta_n) = 0$ has three positive roots, $\theta_- \le \theta_0 \le \theta_+$. We introduce an inner scaling of (43) defining $Y = \frac{y - y_0}{\epsilon^{1/2}}$. Substituting this into (43) and retaining the leading order terms in ϵ, we obtain

$$\frac{d}{dY}\left(\frac{\frac{d\theta_n}{dY}}{\theta_n}\right) + \frac{H(y_0, \theta_n)}{\theta_n^2} = 0. \tag{49}$$

With the change of variable $w = \ln(\theta_n)$, we can rewrite this as

$$\frac{d^2 w}{dY^2} + F(w, y_0) = 0, \tag{50}$$

where $F(w, y_0) = H(y_0, e^w)e^{-2w}$. Clearly, the function $F(w, y_0)$ has three roots, $w_\pm = \ln(\theta_\pm), w_0 = \ln(\theta_0)$. It is well known [4] that there is a solution to the inner-layer (50) that provides a transition between w_- and w_+ if

$$\int_{w_-}^{w_+} F(w, y_0)dw = 0. \tag{51}$$

Inverting the transformation yields an equivalent requirement in the variable θ_n. An interior layer providing a transition between θ_- and θ_+ can be fit at $y = y_0$ if

$$\int_{\theta_-}^{\theta_+} \frac{H(y_0, \theta_n)}{\theta_n^3} d\theta_n = 0. \tag{52}$$

There is another interior layer solution that can be used to construct solutions. If $y_0 = \frac{1}{2}$ and there are three positive roots of $H(\frac{1}{2}, \theta) = 0$, and if

$$\int_{\theta_-}^{\theta_+} \frac{H(\frac{1}{2}, \theta)}{\theta^3} d\theta < 0, \tag{53}$$

then there is a homoclinic orbit of (49) that approaches θ_+ asymptotically as $Y \to \pm\infty$ and has as its minimal value $\theta = \theta^*$, where $\theta_- < \theta^* < \theta_0$ and

$$\int_{\theta^*}^{\theta_+} \frac{H(\frac{1}{2}, \theta)}{\theta^3} d\theta = 0. \tag{54}$$

The first integral for this trajectory is

$$\frac{1}{2}\left(\frac{d\theta_n}{dY}\right)^2 - \theta_n^2 \int_{\theta_n}^{\theta_+} \frac{H(\frac{1}{2}, \theta)}{\theta^3} d\theta = 0. \tag{55}$$

Now we use this information to construct all the possible single-valued solutions. To do this we pick a value of k, determine the possible single-valued solutions, and then find the appropriate value of G (and y_0 if any) for this solution. There are three different types of solutions.

If $h(\theta) = 0$ has only one positive root and if and $h(\theta)$ is monotone decreasing for θ larger than this root, then the solution of $H(y, \theta_n) = 0$ is unique, for any value of G, as seen in Figure 1 for the curves with $k = 2$ and for $k = 5$. In Figure 2 the solution profiles $\theta_n(y)$ for $k = 5$ are shown for three different values of G.

Since G acts as a y-axis scale factor for these profiles, it is apparent that $\int_0^1 \theta_n(y)dy$ is a monotone decreasing function of G. Thus, there is a unique value of G for which $\int_0^1 \theta_n(y)dy = \hat{\theta}_n$. For the profiles shown in Figure 2, this unique value of G is 4.022.

Similarly, for small values of k, unique solutions can be obtained. For example, Figure 3 shows the solution profile for $k = 2$. Again, since the y-axis for this profile is scaled by G, the unique value of G for which $\int_0^1 \theta_n(y)dy = \hat{\theta}_n$ is easily determined. For the profile in Figure 3, this value is $G = 1.74$.

If the function $h(\theta_n)$ is not monotone decreasing, then there is the possibility of nonunique solutions of $H(y, \theta_n) = 0$. If a (positive) level x can be found so that

$$\int_{\theta_-}^{\theta_+} \frac{x + h(\theta_n)}{\theta_n^3} d\theta_n = 0, \tag{56}$$

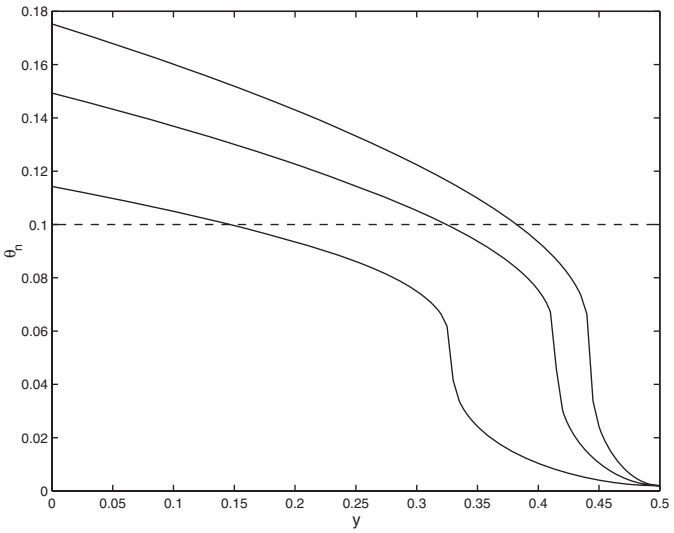

FIG. 2. *Plot of* $\theta_n(y)$ *for* $k = 5$ *and* $G = 2, 4.022, 6$. *Other parameter values are* $\kappa = 20{,}000$ *and* $\theta_{ref} = \hat{\theta}_n = 0.1$.

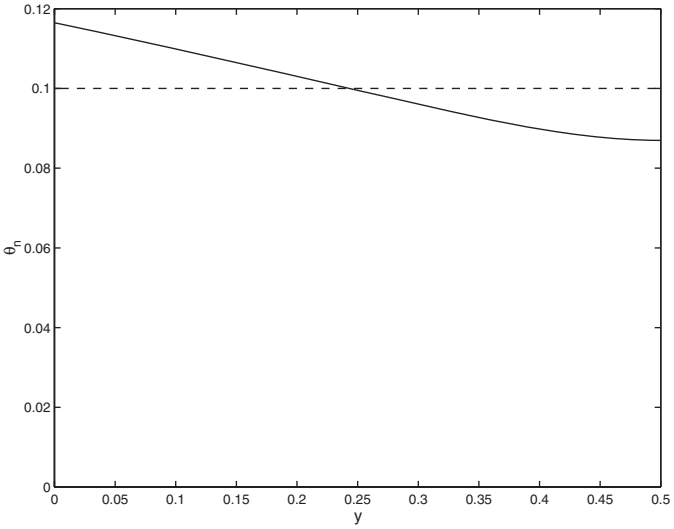

FIG. 3. *Plot of* $\theta_n(y)$ *for* $k = 2$ *and* $G = 1.74$. *Other parameter values are* $\kappa = 20{,}000$ *and* $\theta_{ref} = \hat{\theta}_n = 0.1$.

then a boundary layer can be inserted into the profile at $y_0 = \frac{1}{2} \pm \frac{\sqrt{x}}{G}$, and this boundary layer can be used to connect the largest solution of $H(y_0, \theta_n) = 0$ with the smallest. A plot of a profile that results is shown in Figure 4.

Notice that for this value of k (=2), there are three possible solution profiles, one with no interior layer (shown in Figure 3), one with a boundary layer (shown in Figure 4), and one with a symmetric boundary layer located at $y_0 = \frac{1}{2}$. In the limit that $\epsilon \to 0$, the third of these looks identical to the profile shown in Figure 3, with the exception that θ_n is discontinuous at $y = \frac{1}{2}$, with $\theta_n(\frac{1}{2}) = \theta^*$ defined in (54). The

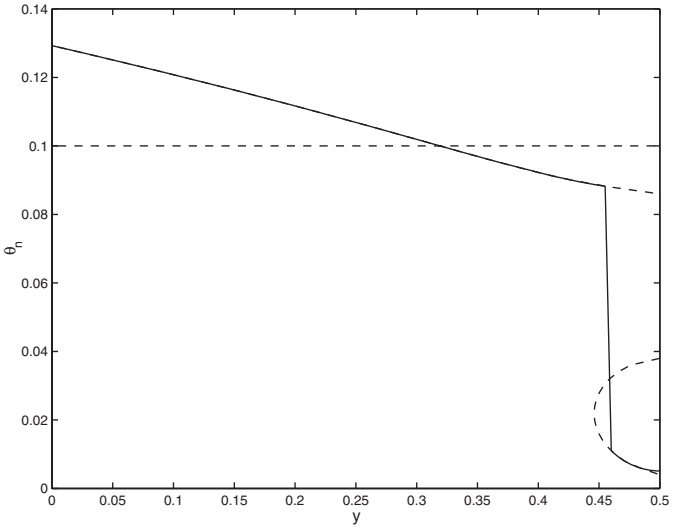

FIG. 4. *Plot of $\theta_n(y)$ for $k = 2$ and $G = 2.47$ with a boundary layer inserted at $y_0 = 0.46$. The dashed curves show all possible solutions of $H(y, \theta_n) = 0$. Other parameter values are $\kappa = 20{,}000$ and $\theta_{ref} = \hat{\theta}_n = 0.1$.*

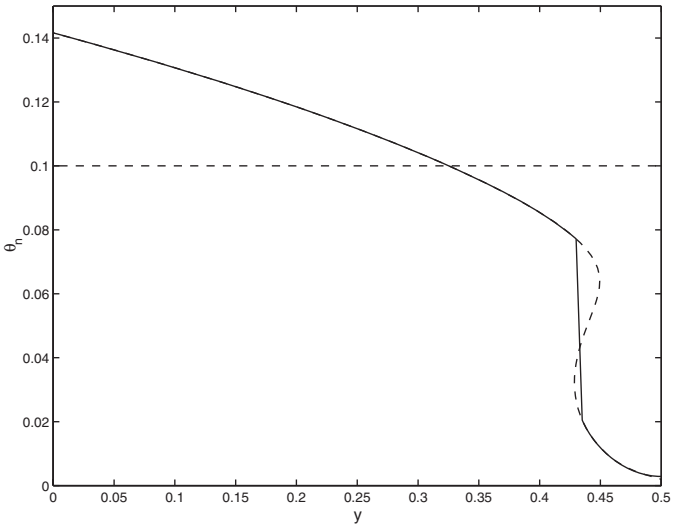

FIG. 5. *Plot of $\theta_n(y)$ for $k = 3.5$ and $G = 3.39$ with a boundary layer inserted at $y_0 = 0.43$. The dashed curves show all possible solutions of $H(y, \theta_n) = 0$. Other parameter values are $\kappa = 20{,}000$ and $\theta_{ref} = \hat{\theta}_n = 0.1$.*

value of G for the first and third solution profiles is the same, but it differs from the value of G for the second transition-layer profile. For some values of k, the boundary layer profile is the only possible solution. A profile of this type occurs for $k = 3.5$ and is shown in Figure 5.

In this way, for each value of k we determine all possible solutions and their corresponding values of G. A plot of the relationship between k and G is shown in Figure 6. Here we see two curves. The lower curve that extends from $k = 0$ to

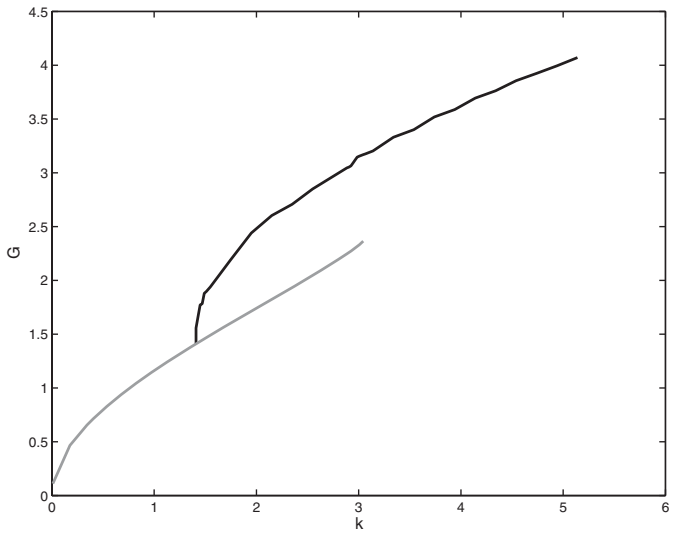

FIG. 6. *Plot of G versus k for the solutions of the gel-flow problem. For this plot, $\kappa = 20{,}000$ and $\theta_{ref} = \hat{\theta}_n = 0.1$.*

$k = 2.9$ corresponds to solutions like those shown in Figure 3 , with no boundary layer. The upper curve that extends from the lower curve at about $k = 1.4$ (with $y_0 = \frac{1}{2}$) corresponds to channeled solutions, with a boundary layer as shown in Figures 4 and 5 for $k < 5$. These solutions merge smoothly into non–boundary layer solutions, such as those shown in Figure 2, as k increases.

The nature of the bifurcation structure of these solutions is not apparent from Figure 6. This is because, for values of k larger than the merger point, the lower branch corresponds to two different solutions. The easier way to visualize this difference is seen in Figure 7, where $\theta_n(\frac{1}{2})$ is plotted as a function of G. Here, the upper solution branch corresponds to those solutions with no boundary layers, the lower solution branch corresponds to those with interior transition layers, and the middle branch (shown dashed) gives the solutions with a symmetric boundary layer at $y = \frac{1}{2}$. In the limit $\epsilon \to 0$, this boundary layer has no thickness and so has no influence on the integral of θ_n. Here we see that the solution is an S-shaped curve, and the bifurcations are via limit points.

The physically significant feature of these curves is that for some values of G there are two physically realizable solutions, a boundary layer, or channeled, solution and a nonchanneled solution. The solution with a boundary layer at $y = \frac{1}{2}$ is transitional between the two and is interesting for mathematical reasons but is unstable and hence not physically realized. Thus, the solution of the gel-flow problem is not unique and exhibits hysteretic behavior, with a hysteresis loop between channeled and nonchanneled solutions, governed by the pressure gradient G.

The behavior of the fluid flow through these two different solution types is understandably different, as the channeled solution permits a higher flux for the same cost. This is illustrated by Figure 8, where the flux of solvent,

$$J = \int_0^1 V_s dy = \frac{1}{h_f} \int_0^1 \frac{1 - \theta_n}{\theta_n} dy, \tag{57}$$

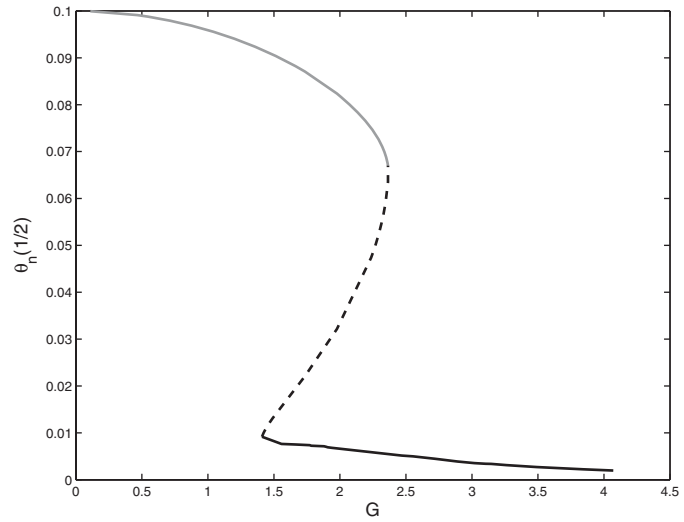

FIG. 7. *Plot of* $\theta_n(\frac{1}{2})$ *versus* G *for the solutions of the gel-flow problem. For this plot,* $\kappa = 20{,}000$ *and* $\theta_{ref} = \hat{\theta}_n = 0.1$.

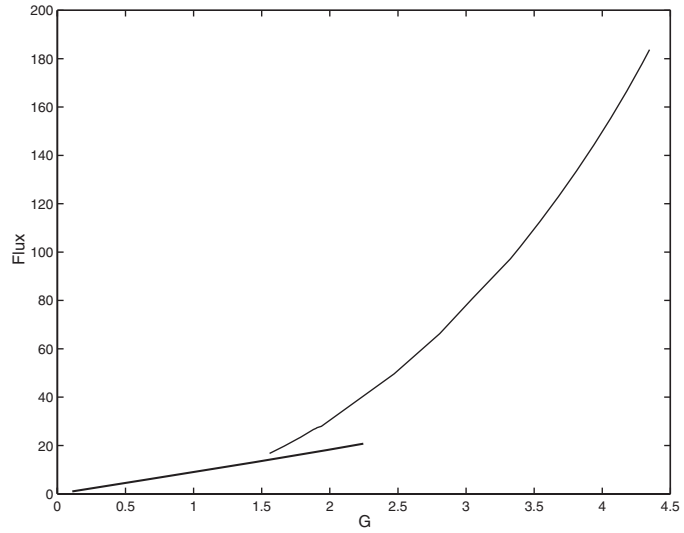

FIG. 8. *Plot of solvent flux as a function of* G. *For this plot,* $\kappa = 20{,}000$ *and* $\theta_{ref} = \hat{\theta}_n = 0.1$.

is plotted as a function of G for the two different solution types. Not surprisingly, if two solutions are possible for the same value of G, the boundary layer solution permits a larger solvent flux than the non–boundary layer solution.

4. Discussion. From this analysis we can deduce the physical mechanism that underlies the formation of channels in a gel. If the osmotic force is sufficiently strong compared to the elastic restoring force, then under a sufficiently high pressure gradient, it is energetically favorable to compress the gel near the wall and swell the gel in the interior, thereby forming a low-resistance channel.

This same conclusion is correct for all gels for which there are two stable gel

concentrations. That is, if $\Psi(\theta_n)$ is such that $\Psi'(\theta_n) < 0$ for $0 \leq \theta_* < \theta_n < \theta^* < 1$ and is positive elsewhere, then if the uniform gel distribution has $\hat{\theta}_n > \theta^*$ and if the osmotic force is sufficiently strong compared to the elastic force, channels will form under sufficiently high pressure gradient flows. This follows from the analysis of the previous section, which relied entirely upon the generic "cubic" shape of the function $\Psi(\theta_n)$ and not on its details. Any function $\Psi(\theta_n)$ with similar structure will lead to the same bifurcation channeling behavior.

REFERENCES

[1] R. B. Bird, R. C. Armstrong, and O. Hassager, *Dynamics of Polymeric Liquids*, Vol. 1, John Wiley and Sons, New York, 1987.

[2] N. G. Cogan and J. P. Keener, *The role of the biofilm matrix in structural development*, Math. Medicine and Biol., 21 (2004), pp. 147–166.

[3] X. He and M. Dembo, *On the mechanics of the first cleavage division of the sea urchin egg*, Exper. Cell Res., 233 (1997), pp. 252–273.

[4] J. P. Keener *Principles of Applied Mathematics: Transformation and Approximation*, Addison–Wesley, Reading, MA, 1988.

[5] A. Kumar and R. K. Gupta, *Fundamentals of Polymers*, chaps. 8 and 9, McGraw–Hill, New York, 1998.

[6] S. R. Lubkin and T. Jackson, *Multiphase mechanics of capsule formation in tumors*, J. Biomech. Eng., 124 (2002), pp. 237–243.

[7] S. T. Milner, *Dynamical theory of concentration fluctuations in polymer-solutions under shear*, Phys. Rev. E, 48 (1993), pp. 3674–3691.

[8] M. Strathmann, T. Griebe, and H.-C. Flemming, *Agarose hydrogels and EPS models*, Water Sci. Technol., 43 (2001), pp. 169–175.

[9] H. Tanaka, *Viscoelastic model of phase separation*, Phys. Rev. E, 56 (1997), pp. 4451–4462.

[10] H. Tanaka, *Viscoelastic phase separation*, J. Phys. Condens. Matter, 12 (2000), pp. R207–R264.

[11] T. Tomari and M. Doi, *Hysteresis and incubation in the dynamics of volume transitions of spherical gels*, Macromolecules, 28 (1995), pp. 8334–8343.

[12] J. Wingender, T. R. Neu, and H.-C. Flemming, *Microbial Extracellular Polymeric Substances. Characterization, Structure and Function*, Springer, New York, 1999.

[13] C. Wolgemuth, E. Hoiczyk, D. Kaiser, and G. Oster, *How myxobacteria glide*, Current Biol., 12 (2002), pp. 369–377.

[14] C. W. Wolgemuth, E. Hoiczyk, and G. Oster, *How gliding bacteria glide*, Biophys. J., 82 (2002), p. 1956.